

Nonperturbative Corrections to the Dilepton Cross Section

Lyndon Alvero

*Institute for Theoretical Physics
State University of New York at Stony Brook
Stony Brook, NY 11794-3840*

December 1994

Abstract

We study the sensitivity of the dilepton production cross section to higher twist terms. A method for calculating the resummed cross section is introduced in moment space, where the leading higher twist terms can be easily parametrized and calculated. We find that a $1/Q$ power correction may significantly affect the cross section at fixed-target energies.

1 Introduction

Large perturbative corrections are common in hadron-hadron scattering cross sections in QCD [1]. In this paper, we will discuss corrections associated with soft gluons that produce large threshold effects. In the case of dilepton production cross sections, such large corrections arise when most of the partonic momenta is carried off by the lepton pair. We will exhibit a class of related nonperturbative corrections that can also have a significant impact on this cross section.

Several methods for resumming threshold corrections have been developed [2]. Recently, resummed cross sections for dilepton production at fixed-target energies have been calculated [3, 4] in principal value resummation (PVR) [5, 6]. In this scheme, the large corrections exponentiate into leading and next-to-leading exponents, E_L and E_{NL} , respectively. These exponents contain the effects of the one- (E_L) and two-loop (E_{NL}) anomalous dimensions and running coupling, and are each defined by a principal value integration. Moreover, because singularities associated with the infrared (IR) behavior of the QCD running coupling are avoided, no explicit IR cutoffs need to be imposed in principal value resummation. An analysis of perturbative resummation [6, 7] shows the presence of nonperturbative power suppressed (higher twist) contributions beginning at $\mathcal{O}(1/Q)$.

It was found in [4] that for protons on fixed-targets, the resummed hard part (in PVR) when combined with parton distributions from global fits led to cross sections that overestimate the data by roughly 30 to 50%. It was also observed in [4] that the discrepancy could be due to higher twist effects. The aim of this paper is to explore this possibility.

In order to analyze the sensitivity of principal value resummation to higher twist effects, we introduce a technique for calculating cross sections which exploits the exponentiation of large corrections in moment-space. We shall show below that to a good approximation, the partonic flux may be approximated by a polynomial in $z = Q^2/\hat{s}$, with Q the pair mass and \hat{s} the partonic center-of-mass invariant mass squared. In this method, the resummed cross section becomes a simple and finite sum of exponentials with coefficients that are functions of energy alone, and most importantly, in which the higher twist effects are easily parametrized and calculated.

The paper is organized as follows: in section 2, we describe in detail how we calculate the resummed cross section in moment space. Here, we will focus only on mass-rapidity distributions at zero rapidity, although our technique can be applied to other distributions as well. In section 3, we present numerical results and compare with experiment. We will find that the resulting resummed cross section in moment space, combined with terms proportional to M/Q , is sensitive to M of the order of hundreds of MeV. Indeed, we find good agreement with data when $M \sim -1$ GeV, for which the higher twist contribution effectively cancels the effects of perturbative resummation. This, in effect, confirms that the cross section may be quite sensitive to higher twist, at least for fixed-target energies. Finally, in section 4, we give a summary and conclusions. Some numerical details are discussed in an appendix.

2 The cross section in moment-space

Schematically, the dilepton-production reaction is given by

$$h_1(p_1) + h_2(p_2) \rightarrow \bar{l}l(Q^\mu) + X, \quad (1)$$

where Q^2 is the lepton-pair mass squared. We will use the standard notation $s = (p_1 + p_2)^2$ and $\tau = Q^2/s$.

At fixed-target energies, where the Z boson may be neglected, principal value resummation provides the following expression (in the DIS scheme), for the differential cross section in dilepton production at zero rapidity, [4]

$$\left. \frac{d^2\sigma}{dQ^2 dy} \right|_{y=0} \simeq \sigma_B(Q^2) \sum_f e_f^2 \int_\tau^1 dz \omega_{f\bar{f}}(z, \alpha) \frac{\mathcal{F}_{f\bar{f}}^{y=0}(\tau/z)}{z}, \quad (2)$$

with

$$\sigma_B(Q^2) = \frac{4\pi\alpha_e^2}{9Q^2 s}, \quad (3)$$

$$\omega(z, \alpha) = A(\alpha) \left(\delta(1-z) - \left[e^{E(\frac{1}{1-z}, \alpha)} \frac{\sin[\pi P_1(\frac{1}{1-z}, \alpha)] \Gamma(1 + P_1(\frac{1}{1-z}, \alpha))}{\pi(1-z)} \right]_+ \right), \quad (4)$$

$$\mathcal{F}_{f\bar{f}}^{y=0}(\tau/z) = F_{f/h_1}(\sqrt{\tau/z}, Q) F_{\bar{f}/h_2}(\sqrt{\tau/z}, Q). \quad (5)$$

The sum in eq. (2) is over all active quark and anti-quark flavors, α_e is the (electromagnetic) fine structure constant, α is proportional to the QCD running coupling (see eq. (10) below) and $F_{f/h}(x, Q)$ denotes the parton distributions. The function $A(\alpha)$, which involves the resummation of large, z -independent Sudakov terms, is given explicitly in appendix A, while we define

$$P_1(x, \alpha) = \frac{d}{dx} E(x, \alpha). \quad (6)$$

The function $E(z, \alpha)$, which exponentiates the large corrections, is, as mentioned above, given as a sum of leading and nonleading contributions. In moment-space, it takes the form

$$E(n, \alpha) = E(n, \alpha)_L + E(n, \alpha)_{NL}. \quad (7)$$

The leading exponent is given explicitly by [6]

$$E(n, \alpha)_L = \alpha(g_1^{(1)} I_1 - g_2^{(1)} I_2), \quad (8)$$

with

$$\begin{aligned} I_1(n, t) &\equiv 2I(n, t/2) - I(n, t), \\ I(n, t) &= t \int_P d\zeta \left(\frac{\zeta^{n-1} - 1}{1 - \zeta} \right) \ln(1 + (1/t) \ln(1 - \zeta)), \\ I_2(n, t) &\equiv \int_P d\zeta \left(\frac{\zeta^{n-1} - 1}{1 - \zeta} \right) \frac{1}{1 + (1/t) \ln(1 - \zeta)}, \end{aligned} \quad (9)$$

where

$$\alpha \equiv \alpha_s(Q^2)/\pi, \quad t \equiv 1/(\alpha b_2), \quad (10)$$

with

$$b_2 = (11C_A - 2n_f)/12. \quad (11)$$

It will be sufficient to consider only the leading exponent $E(n, \alpha)_L$ in the following discussion. For completeness, however, we have reproduced the explicit form of the next-to-leading exponent $E(n, \alpha)_{NL}$, as well as the constants $g_1^{(1)}, g_2^{(1)}$ (eq. (8)) in appendix A.

We are now ready to discuss the higher twist corrections to the resummed cross section $d^2\sigma/dQ^2 dy|_{y=0}$ (eq. (2)). To do so, it will be necessary to go to moment- or n -space, where the resummed hard part of eq. (4) takes the simple form

$$\begin{aligned} \tilde{\omega}_{f\bar{f}}(n, \alpha) &\equiv \int_0^1 dz z^{n-1} \omega_{f\bar{f}}(z, \alpha) \\ &= A(\alpha) e^{E(n, \alpha)}, \end{aligned} \quad (12)$$

with $E(n, \alpha)$ given by eqs. (7-9) and $A(\alpha)$ by eq. (31) of appendix A.

The leading higher twist term implied by the resummed exponent $E(n, \alpha)$ is of the form [6, 7]

$$n \frac{\Lambda}{Q}. \quad (13)$$

This can be derived in the following way [6]. Consider the leading exponent $E(n, \alpha)_L$, which depends on I_1 and I_2 (eq. (9)). By a change of variables, $\ln(1 - \zeta) \rightarrow x'$, and using

$$(1 - r)^{n-1} - 1 = \sum_{m=1}^{\infty} \frac{(1-n)_m}{m!} r^m, \quad (14)$$

where $(a)_m \equiv \Gamma(a+m)/\Gamma(a)$ is the Pochhammer symbol, $I(n, t)$ in eq. (9) can be rewritten as

$$I(n, t) = t \sum_{m=1}^{\infty} \frac{(1-n)_m}{m!} \mathcal{P} \int_{-\infty}^0 dx' e^{mx'} \ln(1 + x'/t), \quad (15)$$

where \mathcal{P} denotes a principal value integration. After several more simple steps, one obtains

$$I(n, t) = - \sum_{m=1}^{\infty} \frac{(1-n)_m}{m! m^2} \mathcal{E}(mt), \quad (16)$$

where the function \mathcal{E} is proportional to the exponential integral function:

$$\mathcal{E}(x) \equiv x e^{-x} \mathcal{P} \int_{-\infty}^x dy \frac{e^y}{y}. \quad (17)$$

Similarly, it can easily be shown that [6]

$$I_2(n, t) = \sum_{m=1}^{\infty} \frac{(1-n)_m}{m! m} \mathcal{E}(mt). \quad (18)$$

The leading higher twist term of $E(n, \alpha)$ comes from the $2\alpha g_1^{(1)} I(n, t/2)$ term that appears in eq. (8). Taking only the leading ($m = 1$) term in the sum in eq. (16), we get

$$2\alpha g_1^{(1)} I(n, t/2) \sim \left(n \frac{\Lambda}{Q}\right) \mathcal{P} \int_{-\infty}^{t/2} dy \frac{e^y}{y}, \quad (19)$$

where we have used the 1-loop form of α , so that t (eq. (10)) is simply, $t = \ln Q^2/\Lambda^2$. Since the pole of the integrand is at $y = 0$, independent of Q , the basic structure of the leading power correction to $E(n, \alpha)$ is $1/Q$. This argument is specific to principal value resummation, but the result is quite general, as discussed in [7], where it was also shown that this power correction is actually induced by the leading infrared renormalon [8].

We now digress on the issue of including higher twist terms in momentum- or z - space. With the correspondence [9]

$$n \leftrightarrow \frac{1}{1-z}, \quad (20)$$

the leading power correction can be parametrized by making the substitution

$$E(z, \alpha) \rightarrow E(z, \alpha) - \frac{c}{1-z} \frac{\Lambda}{Q}, \quad (21)$$

for some constant c , in eq. (4). We then find that the direct calculation of the resummed cross section given by eq. (2) is hopeless, because an essential singularity in $\omega_{f\bar{f}}(z, \alpha)$ (eq. (4)) will be generated at $z = 1$. This highlights one of the advantages of working in n -space, for, as we shall now see, the higher twist term (eq. (13)) is in a form that makes it easy to calculate its effects in the resummed cross section.

To write the cross section in terms of moments, we first need to express the sum involving the parton luminosity as a polynomial in z :

$$\sum_f e_f^2 \mathcal{F}_{f\bar{f}}^{y=0}(\tau/z) \equiv \sum_{n=1}^{n_{max}} C_n(\tau) z^n + \Delta\mathcal{F}(\tau, z), \quad (22)$$

where $\Delta\mathcal{F}$ denotes the error in the polynomial approximation. Some details on how n_{max} is determined, as well as how the interpolating polynomial is obtained, are described in appendix B.

Using eq. (22) in eq. (2), we obtain

$$\left. \frac{d^2\sigma}{dQ^2 dy} \right|_{y=0} \simeq \sigma_B(Q^2) \sum_{n=1}^{n_{max}} C_n(\tau) \int_{\tau}^1 dz z^{n-1} \omega_{f\bar{f}}(z, \alpha) + \sigma_B(Q^2) \int_{\tau}^1 dz \omega_{f\bar{f}}(z, \alpha) \frac{\Delta\mathcal{F}(\tau, z)}{z}. \quad (23)$$

Combining eqs. (12) and (23), and applying several straightforward manipulations, we find

$$\left. \frac{d^2\sigma}{dQ^2 dy} \right|_{y=0} \simeq \sigma_B(Q^2) A(\alpha) \sum_{n=1}^{n_{max}} C_n(\tau) e^{E(n, \alpha)} + CT_1 + CT_2. \quad (24)$$

The explicit forms of the correction terms CT_1 and CT_2 will be given shortly. To study the sensitivity of eq. (24) to higher twist, we insert a term proportional to $n\Lambda/Q$ in the exponent, so that now the n -space resummed cross section is given by

$$\left. \frac{d^2\sigma}{dQ^2 dy} \right|_{y=0} \simeq \sigma_B(Q^2) A(\alpha) \sum_{n=1}^{n_{max}} C_n(\tau) \exp\left[E(n, \alpha) - \frac{cn\Lambda}{Q}\right] + CT_1 + CT_2, \quad (25)$$

where Λ is the QCD scale, c is a constant, and the correction terms are

$$\begin{aligned}
CT_1 &= \sigma_B(Q^2) \int_{\tau}^1 dz \omega_{f\bar{f}}(z, \alpha) \frac{\Delta\mathcal{F}(\tau, z)}{z}, \\
CT_2 &= \sigma_B(Q^2) A(\alpha) \sum_{n=1}^{n_{max}} C_n(\tau) \int_0^{\tau} dz z^{n-1} e^{E(z, \alpha)} \frac{\sin[\pi P_1(z, \alpha)] \Gamma(1 + P_1(z, \alpha))}{\pi(1-z)}, \quad (26)
\end{aligned}$$

with¹ $\omega_{f\bar{f}}(z, \alpha)$ given by eq. (4), and

$$\frac{\Delta\mathcal{F}(\tau, z)}{z} = \sum_f e_f^2 \frac{\mathcal{F}_{f\bar{f}}^{y=0}(\tau/z)}{z} - \sum_{n=1}^{n_{max}} C_n(\tau) z^{n-1}. \quad (27)$$

We will use eq. (25) to calculate resummed cross sections in the next section. Note that in this form, the cross section is simply a finite sum of exponentials weighted by the coefficients of the interpolating polynomial, up to corrections (CT_1 and CT_2) which are expected to be very small, since $\Delta\mathcal{F}(\tau, z)$ is small.

3 Numerical results

For our numerical calculations, we chose to work with the kinematics of the E605 experiment [10], which studied proton beam interactions with a copper target at $\sqrt{s} = 38.8$ GeV. We have used the CTEQ2D distributions with Λ at 4(5) flavors equal to 0.235(0.155) GeV. We have also included all finite 1-loop contributions (see [4]) in all the resummed cross sections that we are now going to present. In the discussions to follow, we will simply denote the cross section $d^2\sigma/dQ^2 dy|_{y=0}$ by σ . Hence, $\sigma(n_{max}, c\Lambda)$ will refer to the cross sections computed in n -space from eq. (25) as described above, for a given n_{max} and $c\Lambda$, and σ_z the cross section computed by the usual method as an integral over z (eq. (2)) with no explicit higher twist, at the same value of Q . We also point out that the cross section defined by eq. (25) is dominated by the sum over n , with the correction terms giving a contribution of not more than 1.6%.

To determine n_{max} , we used the method described in [11]. The basic idea is that by adding a z^{n+1} term to a degree- n polynomial fit to a particular set of data (the parton luminosity (eqs. (5, 22))), the deviation of the interpolation from the data is decreased. However, for some degree n_{max} , the addition of higher powers of z no longer decreases the deviations by a statistically significant amount. We have found that for the data points with which we compare, n_{max} ranges from 13 to 16 only. We also mention that, although the choice of z_{min} , which defines the range of validity of the interpolation (see appendix B), somewhat affects the value of n_{max} , we have verified that the n -space resummed cross section is insensitive to z_{min} . That is, $\sigma(n_{max}, c\Lambda) \simeq \sigma(n'_{max}, c\Lambda)$, where $n_{max}(n'_{max})$ is obtained when $z_{min}(z'_{min})$ is used in the interpolation.

We plot in fig. 1 the resummed cross sections calculated in moment-space and scaled relative to the corresponding z -space cross sections taken from the resummed curve (solid line in fig. 2). The points denoted by circles, triangles and squares correspond to n -space

¹Note that for brevity, we have represented the $1/(1-z)$ dependence of the functions in CT_2 as simply z .

cross sections calculated using eq. (25) with $c\Lambda$ equal to 0, 0.5 and 1 GeV, respectively [recall that we take $c = 0$ for σ_z].

We see that the n -space resummed cross section $\sigma(n_{max}, 0)$ is different from the z -space cross section σ_z . The two differ, however, by no more than 12%, with $\sigma(n_{max}, 0)$ initially smaller but eventually becoming larger than σ_z . This difference already illustrates the range of sensitivity to higher twist effects that are implicit in any resummation prescription. We can also infer from fig. 1 that for $c\Lambda = 1(0.5)$ GeV, the higher twist effects are about 27 to 23% (14 to 11%) of the resummed cross section $\sigma(n_{max}, 0)$, decreasing with τ .

In fig. 2, we plot the data of experiment E605 and reproduce the curves of fig. 9d of [4] (dashed curve=2-loop and solid line=resummed cross section). For comparison, we also include the results obtained for $\sigma(n_{max}, 1\text{GeV})$ (dotted curve). We see that, with this value of $c\Lambda$, the n -space resummed cross section gives quite a good fit to the data for this range of τ . In fact, the $\sigma(n_{max}, 1\text{GeV})$ curve is almost identical to the 1-loop curve in fig. 9d of [4].

4 Discussions and conclusions

In this paper, we have derived an expression in moment-space for the cross section in principal value resummation. In this form, the cross section becomes a finite sum of exponentials, and higher twist terms can be included in an easy, straightforward manner. This is in contrast with the resummation formula written in momentum- or z -space, where it is not possible to treat the higher twist in an analogous fashion.

Direct comparison with experiment shows that a $1/Q$ correction, with a coefficient of order 1 GeV, in this variant form of principal value resummation, agrees with experiment, while the purely perturbative resummed cross sections in [4] overestimate the data. It seems that such a higher twist term is large enough to cancel the effects of resummation, bringing down the resummed cross section to the size of the 1-loop cross section. We also note that this size of the higher twist is comparable to those found in e^+e^- event shape variables [12].

We also mention that for the particular distribution we are concerned with, $d^2\sigma/dQdy|_{y=0}$, it was found in [13] that already at $\mathcal{O}(\alpha_s)$, the non-singular terms in the hard part account for about 20% of the total cross section. Although we have included all such 1-loop finite contributions to our resummed cross sections, there is still some uncertainty due to similar non-singular contributions at higher orders. However, since we are mostly concerned with the structure and effects of the leading higher twist term, and not the precise calculation of cross sections, our conclusions are not affected by this uncertainty.

It should be noted that we have not really explained why the higher twist coefficient should be as big as 1 GeV. It could be that it is actually smaller, in which case, the resummed cross section will still overestimate the data but less than the amount found in [4]. The remaining discrepancy could then be explained by the other factors alluded to in [4]: the importance of higher order effects when combining deeply inelastic scattering (DIS) and hadron-hadron data in global fits, the theoretical uncertainty in $A(\alpha)$, and the effects of finite higher order terms in the hard part. Probably, the full cross section comes from a combination of all such effects. Here, however, we have shown that higher twist does play a role.

ACKNOWLEDGMENTS

I would like to thank George Sterman for many valuable discussions, and for his constant support and guidance. I would also like to thank W. L. van Neerven for a helpful discussion. This work is supported in part by the National Science Foundation, under grant PHY 9309888.

Appendix A The functions $E(n, \alpha)_{NL}$ and $A(\alpha)$

Here, we write down the explicit expressions for the functions $E(n, \alpha)_{NL}$ and $A(\alpha)$ which were described in section 2. The next-to-leading exponent $E(n, \alpha)_{NL}$ is given by [3]

$$E(n, \alpha)_{NL} = \alpha(g_1^{(1)} J_1 - g_2^{(1)} J_2) + \alpha^2(g_1^{(2)} K_1 - g_2^{(2)} K_2), \quad (28)$$

with

$$\begin{aligned} J_1 &\equiv (\alpha b_3/b_2) \int_P d\zeta \left(\frac{\zeta^{n-1} - 1}{1 - \zeta} \right) \int_0^\zeta \frac{dy}{1-y} \frac{\ln(1 + (1/t) \ln[(1-\zeta)(1-y)])}{(1 + (1/t) \ln[(1-\zeta)(1-y)])^2}, \\ J_2 &\equiv -(\alpha b_3/b_2) \int_P d\zeta \left(\frac{\zeta^{n-1} - 1}{1 - \zeta} \right) \frac{\ln(1 + (1/t) \ln(1-\zeta))}{(1 + (1/t) \ln(1-\zeta))^2}, \\ K_1 &\equiv - \int_P d\zeta \left(\frac{\zeta^{n-1} - 1}{1 - \zeta} \right) \int_0^\zeta \frac{dy}{1-y} \frac{1}{(1 + (1/t) \ln[(1-\zeta)(1-y)])^2}, \\ K_2 &\equiv \int_P d\zeta \left(\frac{\zeta^{n-1} - 1}{1 - \zeta} \right) \frac{1}{(1 + (1/t) \ln(1-\zeta))^2}, \end{aligned} \quad (29)$$

where α and t are defined in eq. (10). All integrals are evaluated over a principal value contour as defined in [6, 3]. The various constants are given by²

$$\begin{aligned} g_1^{(1)} &= 2C_F, \quad g_2^{(1)} = -\frac{3}{2}C_F, \quad g_1^{(2)} = C_F \left[C_A \left(\frac{67}{18} - \frac{\pi^2}{6} \right) - \frac{5n_f}{9} \right], \\ g_2^{(2)} &= \frac{1}{4} \left[C_F^2 (\pi^2 - \frac{3}{4} - 12\zeta(3)) + C_A C_F (\frac{11}{9}\pi^2 - \frac{193}{12} + 6\zeta(3)) + \frac{C_F}{2} (-\frac{4}{9}\pi^2 + \frac{17}{3}) \right], \\ b_3 &= (34C_A^2 - (10C_A + 6C_F)n_f)/48, \end{aligned} \quad (30)$$

where n_f is the number of flavors, and C_A, C_F are color factors. The parameter b_2 is defined by eq. (11).

We also point out here that in the calculation of E_{NL} for this paper, the term proportional to the integral K_2 was not included. This term, strictly speaking, yields logarithms beyond nonleading order, as defined in [5, 6]. This treatment differs from the calculations in [3, 4], where the same term was kept. However, we have checked that the contribution from the above K_2 term is no more than 1% of the total cross section. In particular, the resummed curve in fig. 2, which excludes the contributions from the K_2 term, is nearly identical to the solid curve of fig. 9d in [4].

The explicit form of $A(\alpha)$, to the same order, is [4]

$$\begin{aligned} A(\alpha) &= \left(1 + 2C_F\alpha + b\alpha^2 \right) \exp \left(\frac{\alpha}{2} C_F \left[\frac{\pi^2}{3} - 3 \right] + \frac{G^{(1)}}{b_2} \ln r + \pi G^{(2)} \frac{\sin \theta}{r} \alpha^2 \right. \\ &\quad \left. + \frac{\gamma_K^{(1)}}{2b_2^2} \frac{1}{\alpha} (\pi b_2 \theta \alpha - \ln r) + \frac{\gamma_K^{(2)}}{2b_2^2} \ln r \right), \end{aligned} \quad (31)$$

²The parameter $g_2^{(2)}$ can be found from Table 1 of [14], where $B^{(2)} = 4g_2^{(2)}$. The relation between the $g_j^{(i)}$ and B^k is described in [5]. The extra factor of 1/4 in eq. (30) is due to our expansion in $\alpha \equiv \alpha_s/\pi$ rather than $\alpha_s/2\pi$ as in [14].

with

$$\begin{aligned}
r &= \left[1 + (\pi b_2 \alpha)^2\right]^{\frac{1}{2}}, \quad \theta = \arctan(\pi b_2 \alpha), \quad G^{(1)} = \frac{3}{2} C_F, \\
G^{(2)} &= C_F^2 \left[\frac{3}{16} - \frac{7}{3} \zeta(3) + \frac{23}{6} \zeta(2) \right] + C_A C_F \left[\frac{2545}{432} + \frac{11}{12} \zeta(2) - \frac{13}{4} \zeta(3) \right] \\
&\quad + n_f C_F \left[-\frac{209}{216} - \frac{1}{6} \zeta(2) \right], \\
\gamma_K^{(1)} &= 2C_F, \quad \gamma_K^{(2)} = C_A C_F \left[\frac{67}{18} - \zeta(2) \right] - \frac{5}{9} n_f C_F,
\end{aligned} \tag{32}$$

and

$$\begin{aligned}
b &= C_F^2 \left[\frac{-23}{720} \pi^4 - \frac{35}{96} \pi^2 + \frac{15}{2} \zeta(3) + \frac{15}{8} \right] + C_A C_F \left[\frac{215}{144} + \frac{175}{216} \pi^2 - \frac{49}{12} \zeta(3) - \frac{17}{1440} \pi^4 \right] \\
&\quad + n_f C_F \left[\frac{1}{3} \zeta(3) - \frac{19}{72} - \frac{7}{54} \pi^2 \right],
\end{aligned} \tag{33}$$

where $\zeta(s)$ is the Riemann Zeta function.

Appendix B Interpolating Polynomials

The interpolating polynomial that we require is defined by eq. (22), repeated below:

$$\sum_f e_f^2 \mathcal{F}_{f\bar{f}}^{y=0}(\tau/z) \equiv \sum_{n=1}^{n_{max}} C_n(\tau) z^n + \Delta \mathcal{F}(\tau, z).$$

For a particular value of Q , we generate a set of values of the left-hand side of the above equation in a certain range of z , $z_{min} < z < 1$. The parameter z_{min} is selected such that $\mathcal{F}_{f\bar{f}}^{y=0}(\tau/z) \sim 0$ for $z < z_{min}$. The typical values of z_{min} that we used vary from 0.075 to 0.2. We then use the Fortran 77 IMSL package on each set of values to obtain the interpolating polynomial, or equivalently, the coefficients $C_n(\tau)$. The polynomials that we obtain fit the luminosity data very well, with percentage differences of the order of 10^{-5} or better.

In principle, given a set of data points, one can always fit a polynomial of degree n_{max} , up to $n_{max} = \text{number of points}$. However, as described in section 3, a method exists for determining a non-trivial n_{max} . One expects that the polynomial can fit the luminosity data very well in the region $z > z_{min}$. Outside this fit region, care must be taken that the selected polynomial does not behave wildly. To be specific, the lowest value that z (or z_{min}) can take is τ , where the luminosity vanishes. It must then be checked that for $z < z_{min}$, the polynomial fits are free of large oscillations. We have verified that the fits we have obtained are indeed well-behaved in this region of z .

FIGURE CAPTIONS

Figure 1. Fractional deviations of the resummed cross section in n -space, $\sigma(n_{max}, c\Lambda)$ (eq. (25)), from the purely perturbative cross section, σ_z (eq. (2)). $c\Lambda = 0$ (circles); $c\Lambda = 0.5$ GeV (triangles); $c\Lambda = 1$ GeV (squares).

Figure 2. Comparison with E605 data. Solid=resummed σ_z ; Dashed=2-loop; Dotted=resummed $\sigma(n_{max}, c\Lambda = 1$ GeV).

References

- [1] G. Altarelli, R.K. Ellis and G. Martinelli, Nucl. Phys. B157 (1979) 461; B. Humpert and W.L. van Neerven, Phys. Lett. B84 (1979) 327; J. Kubar-Andre and F.E. Paige, Phys. Rev. D19 (1979) 221; K. Harada, T. Kaneko and N. Sakai, Nucl. Phys. B155 (1979) 169; B165 (1980) 545 (E); T. Matsuura and W. L. van Neerven, Z. Phys. C38 (1988) 623; T. Matsuura, S.C. van der Marck and W.L. van Neerven, Phys. Lett. B211 (1988) 171.
- [2] G. Sterman, Nucl. Phys. B281 (1987) 310; S. Catani and L. Trentadue, Nucl. Phys. B327 (1989) 323; B353 (1991) 183.
- [3] L. Alvero and H. Contopanagos, ANL-HEP-PR-94-25/ITP-SB-94-33 (July 1994).
- [4] L. Alvero and H. Contopanagos, ANL-HEP-PR-94-59/ITP-SB-94-41 (November 1994).
- [5] H. Contopanagos and G. Sterman, Nucl. Phys. B400 (1993) 211.
- [6] H. Contopanagos and G. Sterman, Nucl. Phys. B419 (1994) 77.
- [7] G.P. Korchemsky and G. Sterman, ITP-SB-94-50 (November 1994).
- [8] G. 't Hooft, in *The whys of subnuclear physics*, Erice 1977, edited by A. Zichichi (Plenum, New York, 1979); A.H.Mueller, in *QCD 20 years later*, Aachen 1992, eds. P.M. Zerwas and H.A. Kastrup (World Scientific, Singapore, 1993).
- [9] G.P. Korchemsky and G. Marchesini, Phys. Lett. B313 (1993) 433.
- [10] G. Moreno et al. (E605 Collaboration), Phys. Rev. D43 (1991) 2815.
- [11] J. Neter, W. Wasserman and M.H. Kutner, *Applied linear regression models* (Richard D. Irwin, Inc., Illinois, 1983) pp.94,300.
- [12] B.R. Webber, Phys. Lett. B339 (1994) 148; A.V. Manohar and M.B. Wise, UCSD/PTH 94-11/CALT-68-1937 (June 1994).
- [13] P.J. Rijken and W.L. van Neerven, INLO-PUB-14/94 (August 1994).
- [14] C.T.H. Davies, B.R. Webber and W.J. Stirling, Nucl. Phys. B256 (1985) 413.

This figure "fig1-1.png" is available in "png" format from:

<http://arxiv.org/ps/hep-ph/9412335v1>

This figure "fig1-2.png" is available in "png" format from:

<http://arxiv.org/ps/hep-ph/9412335v1>

p Cu (38.8 GeV)

E605 (CTEQ2D)

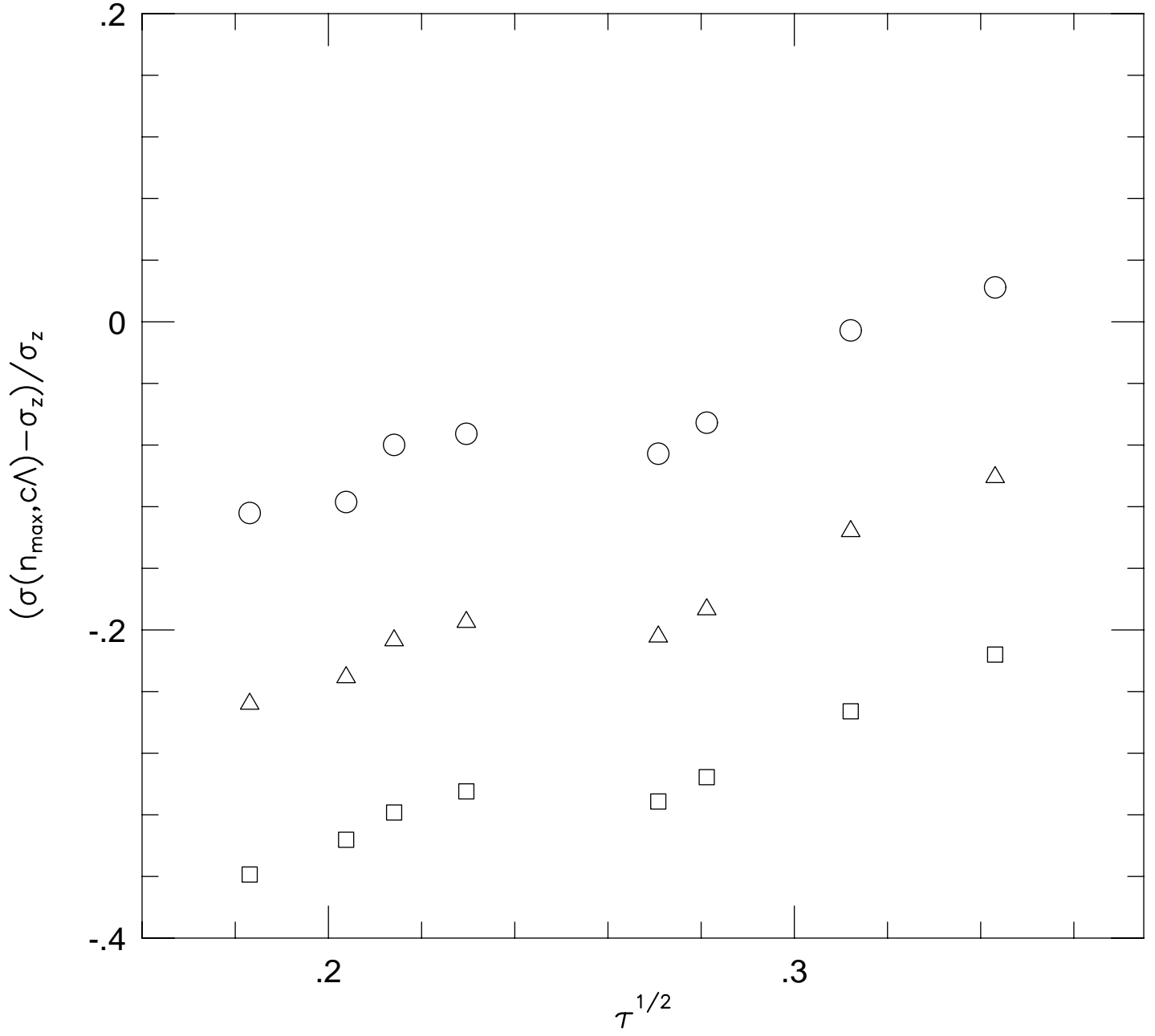


Fig. 1

p Cu (38.8 GeV) CTEQ2D ($\Lambda_4=0.235\text{GeV}$)

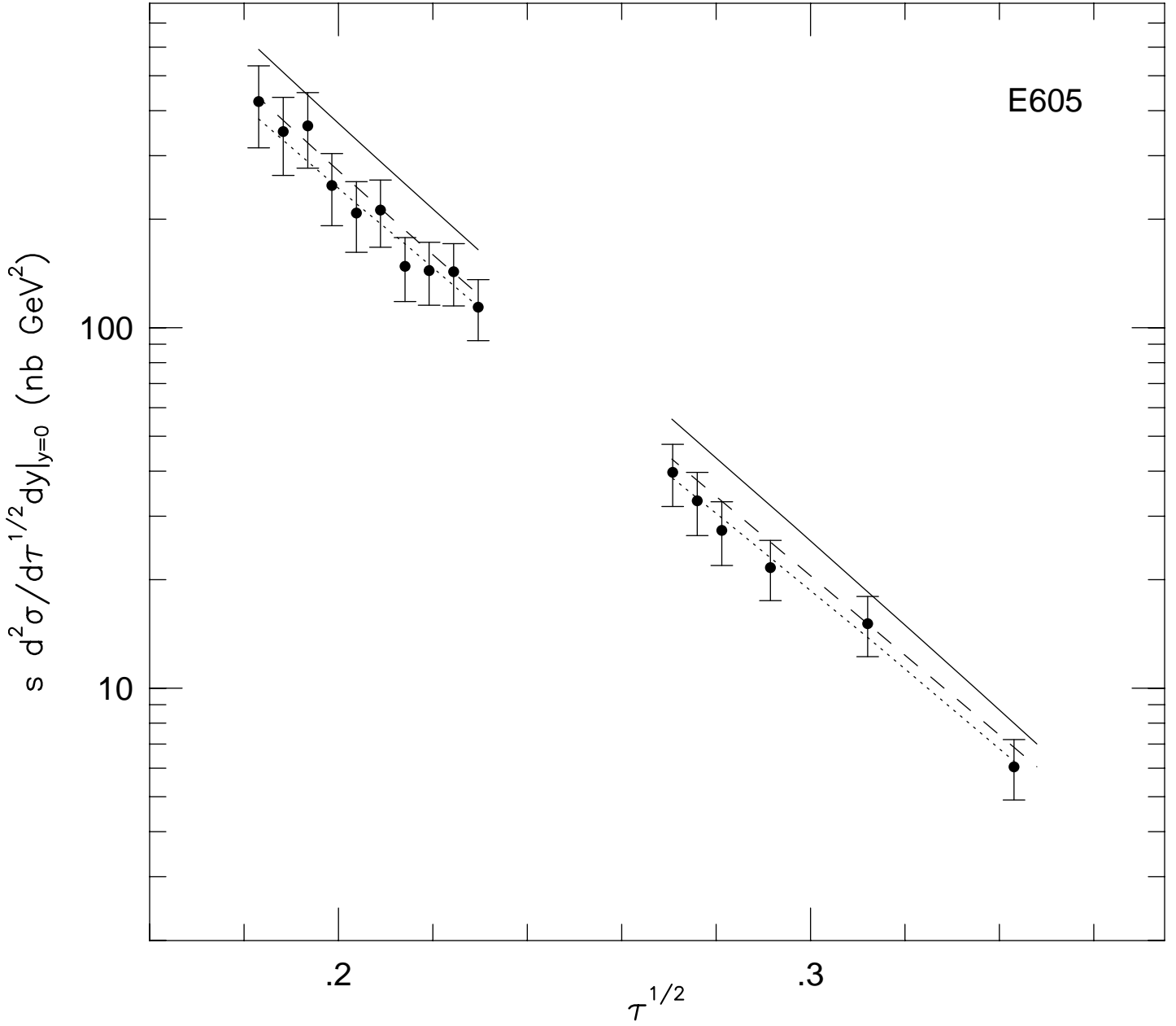


Fig. 2